Oxygen-vacancy-mediated dielectric property in perovskite $Eu_{0.5}Ba_{0.5}TiO_{3-\delta}$ epitaxial thin films

Weiwei Li, Junxing Gu, Qian He, Kelvin H. L. Zhang, Chunchang Wang, Kuijuan Jin, Yongqiang Wang, Matias Acosta, Haiyan Wang, Albina Y. Borisevich, Judith L. MacManus-Driscoll, and Hao Yang

Citation: Appl. Phys. Lett. **112**, 182906 (2018); doi: 10.1063/1.5025607
View online: https://doi.org/10.1063/1.5025607
View Table of Contents: http://aip.scitation.org/toc/apl/112/18
Published by the American Institute of Physics

Oxygen-vacancy-mediated dielectric property in perovskite $Eu_{0.5}Ba_{0.5}TiO_{3-\delta}$ epitaxial thin films

Weiwei Li,[1,2,a)] Junxing Gu,[3] Qian He,[4] Kelvin H. L. Zhang,[5] Chunchang Wang,[6] Kuijuan Jin,[3] Yongqiang Wang,[7] Matias Acosta,[2] Haiyan Wang,[8,9] Albina Y. Borisevich,[4] Judith L. MacManus-Driscoll,[2] and Hao Yang[1,b)]

[1]*College of Science, Nanjing University of Aeronautics and Astronautics, Nanjing 211106, China*
[2]*Department of Materials Science and Metallurgy, University of Cambridge, 27 Charles Babbage Road, Cambridge CB3 0FS, United Kingdom*
[3]*Beijing National Laboratory for Condensed Matter Physics and Institute of Physics, Chinese Academy of Science, Beijing 100190, China*
[4]*Materials Science and Technology Division, Oak Ridge National Laboratory, Oak Ridge, Tennessee 37831, USA*
[5]*Department of Chemical and Biochemical Engineering, College of Chemistry and Chemical Engineering, Xiamen University, Xiamen 361005, China*
[6]*Laboratory of Dielectric Functional Materials, School of Physics and Material Science, Anhui University, Hefei 230039, China*
[7]*Materials Science and Technology Division, Los Alamos National Laboratory, Los Alamos, New Mexico 87545, USA*
[8]*Department of Electrical and Computer Engineering, Texas A&M University, College Station, Texas 77843-3128, USA*
[9]*School of Materials Engineering, Electrical and Computer Engineering, Purdue University, West Lafayette, Indiana 47907, USA*

(Received 11 February 2018; accepted 20 April 2018; published online 2 May 2018)

Dielectric relaxation in ABO_3 perovskite oxides can result from many different charge carrier-related phenomena. Despite a strong understanding of dielectric relaxations, a detailed investigation of the relationship between the content of oxygen vacancies (V_O) and dielectric relaxation has not been performed in perovskite oxide films. In this work, we report a systematic investigation of the influence of the V_O concentration on the dielectric relaxation of $Eu_{0.5}Ba_{0.5}TiO_{3-\delta}$ epitaxial thin films. Nuclear resonance backscattering spectrometry was used to directly measure the oxygen concentration in $Eu_{0.5}Ba_{0.5}TiO_{3-\delta}$ films. We found that dipolar defects created by V_O interact with the off-centered Ti ions, which results in the dielectric relaxation in $Eu_{0.5}Ba_{0.5}TiO_{3-\delta}$ films. Activation energy gradually increases with the increasing content of V_O. The present work significantly extends our understanding of relaxation properties in oxide films. *Published by AIP Publishing.*
https://doi.org/10.1063/1.5025607

Complex ABO_3 perovskite oxides exhibit a broad spectrum of physical properties due to their highly tunable ground states that make them indispensable in oxide electronic devices.[1] The functional properties of perovskite oxides are strongly influenced by composition, defects, and BO_6 octahedral distortions.[2] Among them, oxygen vacancies (V_O) are one of the fundamental and intrinsic defects that affect crucial functionalities such as optical properties,[3,4] superconductivity,[5] magnetism,[6–8] ferroelectricity,[9,10] multiferroicity,[11] resistive switching,[12,13] and ionic conductivity.[14,15]

The low-frequency relaxation properties of perovskite oxides, which are critical for applications in sensors, actuators, transducers, and dynamic random access memories,[16–19] are known to be closely related to V_O. The dielectric properties in the low-frequency regime offer rich information about impurities, defects, and space charge effects. For example, in the $ATiO_3$ (A = Ba, Ca, and Pb) system, V_O create space charge regions at the dielectric/electrode interfaces, inducing dielectric relaxation.[20] Dielectric relaxation phenomena have been reported in La- and Ti-co-doped or La- and Mg-co-doped $BiFeO_3$ and Bi-doped $SrTiO_3$ with the effect attributed to the ionization and movement of V_O.[21–24] Furthermore, the movement of V_O confined at the vertical interfaces and hampered by the misfit dislocations is responsible for the relaxation behavior in nanocomposite $(BaTiO_3)_{1-x}$:$(Sm_2O_3)_x$ films.[25]

It clearly shows that the role of V_O as a complex defect on the relaxation phenomena is very complicated. More detailed work is needed to fully understand the role of V_O on the dielectric relaxation of ABO_3 perovskite oxides, which is both fundamentally interesting and technologically important. Tuning the content of V_O is an ideal way to reveal the relationship between V_O and dielectric relaxation and is also critical for practical applications. However, a systematical investigation of this correlation has not been reported to date, largely due to the difficulties in controlling and determining V_O precisely.

$Eu_{0.5}Ba_{0.5}TiO_3$ (EBTO), an antiferromagnetic-ferroelectric multiferroic material with ferroelectric Curie temperature of 213 K in bulk, is an interesting system for probing dielectric relaxation effects.[8] In $Eu_{0.5}Ba_{0.5}TiO_{3-\delta}$ ($EBTO_{3-\delta}$) films, it has been demonstrated that the introduction of V_O creates Ti^{3+} $3d^1$ defect states, which mediates the ferromagnetic coupling between the localized Eu $4f^7$ spins.[8,11] Also the introduction of

a)Email: wl337@cam.ac.uk
b)Email: yanghao@nuaa.edu.cn

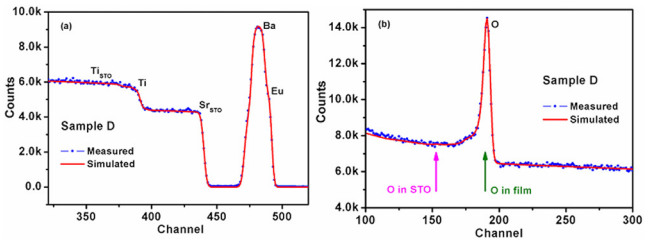

FIG. 1. Stoichiometry and oxygen concentration of Sample D: (a) RBS spectrum and (b) oxygen resonance peak with the simulated curve (red line).

V_O increases the off-center displacement of Ti ions. This enhances the ferroelectric Curie temperature above room temperature, which makes $EBTO_{3-\delta}$ films a promising candidate for memory device applications.[8,11]

In this letter, dielectric permittivity, modulus, and impedance of $EBTO_{3-\delta}$ films were studied as a function of temperature and frequency. Epitaxial $EBTO_{3-\delta}$ films were grown on (001) oriented $SrTiO_3$ (STO) and Nb-doped $SrTiO_3$ (Nb-STO, Nb: 0.5 wt. %) substrates. Details on sample synthesis can be found elsewhere.[8,11] The $EBTO_{3-\delta}$ films, grown at oxygen partial pressure (P_{O_2}) of 1×10^{-1}, 1×10^{-2}, 1×10^{-3}, and 1×10^{-4} Pa, were named as Samples A, B, C, and D, respectively. The crystal structure was investigated by X-ray diffraction (XRD) and scanning transmission electron microscopy (STEM, Nion UltraSTEM 200). Nuclear resonance backscattering spectrometry (NRBS) was performed on 3 MV Pelletron Tandem Accelerator. A sandwich capacitor structure of Pt/$EBTO_{3-\delta}$/Nb-STO with a thickness of ~250 nm was used for electrical measurements. Top Pt electrodes with an area of 8×10^{-4} cm^2 were fabricated by sputtering. The dielectric properties were measured using an Agilent 4294A Impedance Analyzer as a function of temperature from 120 to 350 K and frequency between 1 and 100 kHz. Current-voltage characteristics were measured using a Keithley 6517 analyzer.

Sample D, grown under the lowest P_{O_2} and presumed to have the maximum content of V_O, was chosen for the detailed analysis. Figure S1 shows a typical XRD θ–2θ spectrum, ω-rocking curves, ϕ-scan, and reciprocal space maps (RSMs). The $EBTO_{3-\delta}$ film peaks have the same position as these of Nb-STO substrate, indicative of cubic-on-cubic epitaxy [Fig. S1(d)]. RSMs clearly demonstrate that the $EBTO_{3-\delta}$ film is free from strain [Fig. S1(e)]. Moreover, there is no difference on the q_x and q_z of the $EBTO_{3-\delta}$ peaks and the c/a (c/a: out-of-plane/in-plane lattice constant) ratio is above 1, meaning the structure of the $EBTO_{3-\delta}$ film is tetragonal.

The stoichiometry and oxygen concentration in $EBTO_{3-\delta}$ films were analyzed by Rutherford Backscattering Spectrometry (RBS) and NRBS. A 3.043 MeV $^4He^+$ was used in the measurement. At such beam energy, there is a strong and narrow resonant scattering from oxygen in the $EBTO_{3-\delta}$ films (not in the substrate). Figure 1(a) shows the RBS spectrum measured from Sample D. With the uncertainty of the measurements (~5%), a SIMNRA simulated spectrum overlapped with the measured spectrum determined that the cation ratio in $EBTO_{3-\delta}$ films (Eu: Ba: Ti) is 1:1:2.[26,27] Figure 1(b) shows the measured oxygen scattering spectrum in Sample D along with a SIMNRA fitted oxygen spectrum. A bare STO substrate was also measured to use it as a standard reference and to minimize uncertainties. The concentration of O was estimated to be 2.98, 2.96, 2.91, and 2.85 for Samples A, B, C, and D, respectively. Thus, the content of V_O (δ) is inferred to be 0.02, 0.04, 0.09, and 0.15 for Samples A, B, C, and D (Table SI), respectively.

To investigate the microstructure, aberration-corrected STEM imaging under the high-angle annular dark-field (HAADF) mode was conducted on Sample A (Fig. S2) and Sample D (Fig. 2). HAADF imaging in STEM, also known as Z-contrast imaging,[28] can provide the relative cation displacements of the B-site atoms in the ABO_3 perovskite oxides.[29] Figure 2 shows a high resolution STEM image at the interface between the thin film and the substrate, confirming the heteroepitaxial growth of the $EBTO_{3-\delta}$ thin film on the STO substrate. The inset provides a schematic representation of the quantification method used to determine the cation column positions and relative displacements. The in-plane (d_y) and out-of-plane (d_z) displacements of Ti ions for the $EBTO_{3-\delta}$ thin film and the STO substrate are plotted. The line profiles show that the $EBTO_{3-\delta}$ film features displacement of the Ti ions along in-plane (d_y) and the out-of-plane (d_z) directions. The Ti ions displacement renders a non-centrosymmetric structure, which is a sufficient condition for a material to exhibit piezoelectricity (discarding the point group 432). As shown in the previous study, the domain switching was found in Sample D, indicating that it is indeed a ferroelectric state above room temperature.[11] In contrast, the average of d_y and d_z for Sample A (Fig. S2) is very close to zero, indicating the ferroelectric Curie temperature is below room temperature. Comparing Sample A with Sample D, we find that the off-center displacement of Ti ions is increased with the increasing content of V_O. It can also be seen that the average of d_y and d_z for the STO substrate is around zero, confirming its room temperature paraelectricity.

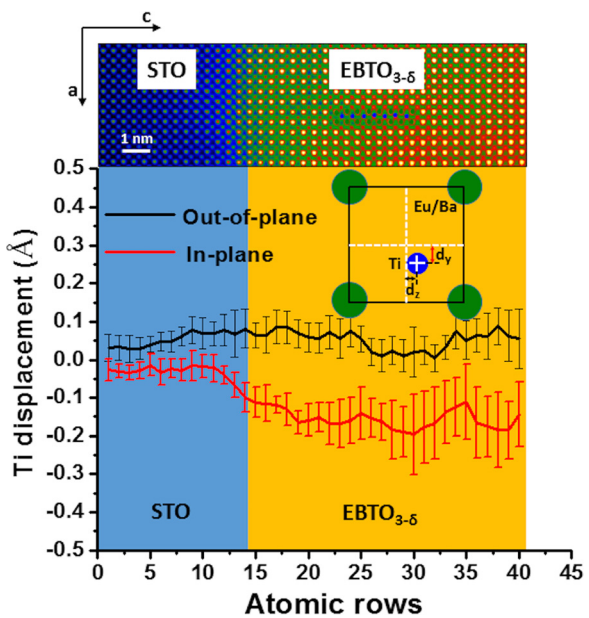

FIG. 2. Top panel: higher magnification HAADF-STEM image of $EBTO_{3-\delta}$ on STO for Sample D. Bottom panel: line profiles of out-of-plane and in-plane displacement of B-site cation (Ti) in the $EBTO_{3-\delta}$ thin film. The inset shows atomic model to illustrate the displacement of B-site cation (Ti) from the center position.

The temperature dependent real part of dielectric permittivity (ε_r') and dielectric loss ($\tan\delta$) for Samples B and D is shown in Fig. 3. Figure S3 shows the results measured from Samples A and C. The temperature profiles of dielectric permittivity, displayed in Figs. 3(a) and 3(c), indicate the presence of frequency-dependent dielectric relaxation peaks for Samples B and D, respectively. The peaks move to higher temperature and their intensity decreases with the increasing frequency. The peaks observed in the $\tan\delta$ curves [Figs. 3(b) and 3(d)] also shift towards higher temperature with increasing frequency. To probe the physical mechanism, the relaxation parameters were calculated by fitting the loss-peak using the Arrhenius law

$$f = f_0 \exp\left(-\frac{E_a}{k_B T_p}\right), \tag{1}$$

where f_0 is the pre-exponential factor, E_a is the activation energy required for the relaxation process, k_B is the Boltzmann constant, and T_p is the temperature where the maximum loss tangent occurs. The Arrhenius plots are presented as insets in Figs. 3(b) and 3(d). The values of E_a and f_0 (Table SI) obtained after the fitting were (0.32 ± 0.02) eV and $(1.89 \pm 0.1)\times10^{10}$ Hz for Sample A, (0.35 ± 0.02) eV and $(2.13 \pm 0.1)\times10^{10}$ Hz for Sample B, (0.40 ± 0.02) eV and $(1.96 \pm 0.1)\times10^{11}$ Hz for Sample C, and (0.44 ± 0.02) eV and $(2.18 \pm 0.1)\times10^{13}$ Hz for Sample D, respectively. Clearly, E_a is increased with the increasing content of V_O (i.e., from Samples A to D).

To further confirm the dielectric relaxation of the $EBTO_{3-\delta}$ films, the electrical modulus (M^*) was introduced. M^* is defined as

$$M^* = M' + jM'' = \frac{1}{\varepsilon^*} = \frac{\varepsilon'}{|\varepsilon|^2} + j\frac{\varepsilon''}{|\varepsilon|^2}. \tag{2}$$

The modulus is the reciprocal of complex dielectric permittivity. Thus, the more conductivity loss contributes to the dielectric permittivity, and the less conductivity loss affects the modulus. Moreover, the modulus also aids in suppressing the electrode polarization effect.[30] The imaginary (M'') part of electrical modulus (M^*) given by $M'' = \varepsilon''/[(\varepsilon')^2 + (\varepsilon'')^2]$ was plotted as a function of temperature, and the results of the fitting were made using the Arrhenius law [Eq. (1)]. The results are presented in Fig. S4 for Samples B and D. As expected, similar to the dielectric permittivity, well-defined frequency-dependent relaxation peaks were found. The relaxation parameters of E_a and f_0 (Table SI) were calculated to be (0.34 ± 0.02) eV and $(8.33 \pm 0.1)\times10^{10}$ Hz for Sample B, (0.42 ± 0.02) eV and $(1.54 \pm 0.1)\times10^{13}$ Hz for Sample D. The E_a obtained from $M''(T)$ is the same as the calculated values from $\tan\delta(T)$, reaffirming the existence of the dielectric relaxation in $EBTO_{3-\delta}$ films.

It is noteworthy that the value of E_a gradually increases with the increasing content of V_O. This means that the dielectric relaxation observed in $EBTO_{3-\delta}$ films is closely related to V_O. Now, we turn to explore the origin of dielectric relaxation in $EBTO_{3-\delta}$ films. Because a sandwich capacitor structure of Pt/$EBTO_{3-\delta}$/Nb-STO was used for dielectric measurements, the dielectric relaxation should be derived from either the $EBTO_{3-\delta}$ films or interfaces between the electrodes and the $EBTO_{3-\delta}$ films. It was reported that V_O gradients at the film/electrode interface affect the fatigue and dielectric loss in ferroelectric oxides.[20,31] In order to distinguish whether the film/electrode interfaces or thin films dominate the relaxation process, the impedance spectra of $EBTO_{3-\delta}$ films were studied. By definition, Z^* is defined as

$$Z^* = Z' - jZ'' = \frac{1}{j\omega C_0 \varepsilon^*}, \tag{3}$$

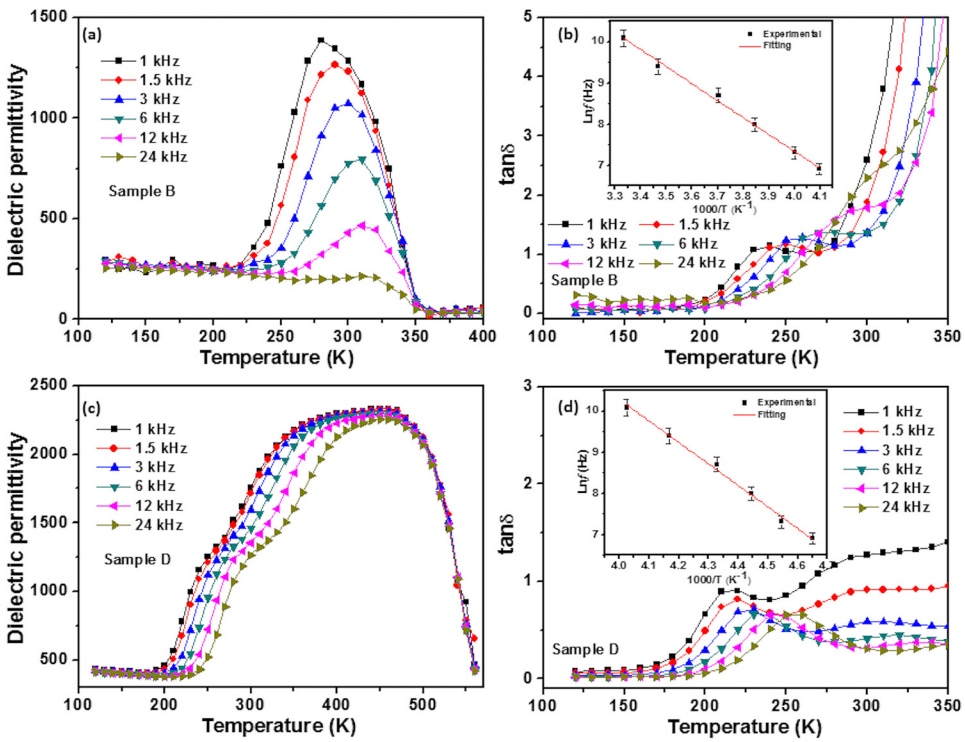

FIG. 3. Temperature dependent dielectric permittivity spectra for Samples B (a) and D (c), dielectric loss ($\tan\delta$) spectra for Samples B (b) and D (d) measured at various frequencies. The insets show the Arrhenius plots of the relaxation. The straight line is the linear fitting result based on the Arrhenius law.

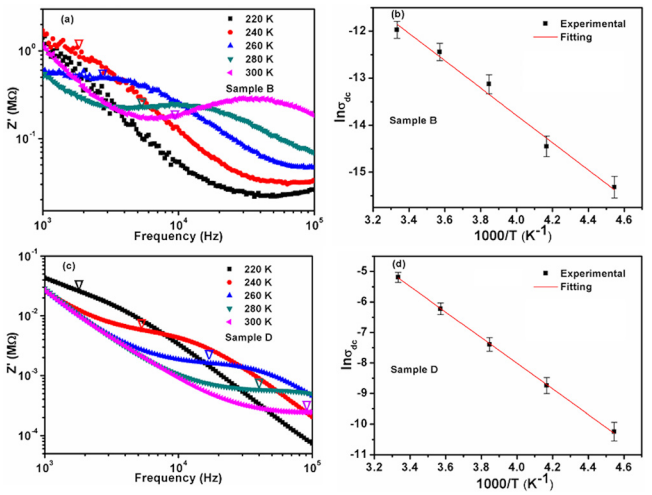

FIG. 4. Frequency dependent real part impedance Z' spectra for Samples B (a) and D (c) measured at various temperatures. The *dc* conductivity is defined from the plateau of Z', as indicated by the triangle. Arrhenius plots of the *dc* conductivities for Samples B (b) and D (d).

where ω is the angular frequency ($\omega = 2\pi f$), $C_0 = \varepsilon_0 S/l$ is the geometrical capacitance with ε_0 being the permittivity of free space (8.854×10^{-12} F/m), l the film thickness, and S the area of each electrode. Z' versus the frequency of Samples B and D at different temperatures is plotted in Figs. 4(a) and 4(c), respectively. Figure S5 shows the results obtained from Samples A and C. The resistance of Sample D is lower than that of Sample B at the same temperature, owing to a higher content of V_O. Furthermore, the magnitude of Z' decreases with increasing frequency and temperature. This implies an increase in *ac* conductivity with increasing frequency and temperature. Temperature dependent Z' flatted regions were found to shift towards higher frequency with increasing temperature. These frequency-independent plateau regions are assigned to the frequency-independent conductivity, suggesting the involvement of dc conductivity. It was also reported that low frequency-independent conductivity and high frequency-dependent conductivity can be assigned to the dc conductivity and the capacitive components of the thin film, respectively.[32,33] Thus, the dc conductivity is defined from the plateau of real part impedance Z', as indicated by the triangle.

Figures 4(b) and 4(d) show the fitted *dc* conductivities for Samples B and D as a function of the reciprocal temperature. The Arrhenius law $\sigma = \sigma_0 \exp(-E_a/k_B T_p)$ was used to fit the curves. σ_0 is the pre-factor, E_a denotes the activation for the response, k_B is the Boltzmann constant, and T_p is the absolute temperature. The activation energies of (0.27 ± 0.02) eV, (0.29 ± 0.02) eV, (0.34 ± 0.02) eV, and (0.37 ± 0.02) eV were obtained for Samples A–D (Table SI), respectively. These values are consistent with the values calculated from the dielectric loss and the electrical modulus, indicating that the dielectric relaxation is mainly derived from the $EBTO_{3-\delta}$ films. The leakage behavior of Samples A–D was also analyzed. A leakage mechanism of trap-controlled space-charge-limited current (SCLC) was determined (Fig. S6). The SCLC is a typical bulk-limited conduction.[34,35] This means that the dielectric relaxation featured in Pt/$EBTO_{3-\delta}$/Nb-STO does arise from the $EBTO_{3-\delta}$ film. It does not derive from the film/electrode interfaces.

Dipolar defects and concomitant local random fields may be a preponderant factor in determining the development of a glassy state or a ferroelectric state, as well as the order of a phase transition in metal oxides.[36] Typical examples of materials in which ferroelectricity can be promoted due to dipolar defects include the $K_{1-x}Li_xTaO_3$, $KTa_{1-x}Nb_xO_3$, and $Sr_{1-x}Ca_xTiO_3$ systems with the high doping content.[37] In these systems, the ferroelectric state results from the off-center nature of the dopant cations (Li^+, Nb^{5+}, and Ca^{2+}). It was also reported that dipolar defects induced by V_O can result in ferroelectricity in either $CaTiO_3$ or $BaZrO_3$.[38,39] In previous work, we demonstrated via first principle calculations that V_O are located nearer to the Ti ions, thereby forming a dipolar defect that generates a local polar distortion.[11]

The strong correlation between the dielectric permittivity and the second harmonic generation signal clearly suggests that the development of a ferroelectric non-centrosymmetric structure is associated with the dielectric relaxation.[11] The idea that the development of a ferroelectric state with a concomitant dielectric relaxation is possible in materials with dipolar defects is well established.[40–42] It was demonstrated both with an experimental and a phenomenological approach that the ferroelectric Curie temperature is enhanced with the increasing dipolar defect concentration.[43] This is in good agreement with our experimental observations.[8,11] Therefore, the development of a dielectric relaxation near the ferroelectric Curie temperature observed in $EBTO_{3-\delta}$ films is a direct consequence of polar clusters originating from the dipolar defects. The percolation of the polar cluster results in the long range ferroelectric order below the Curie temperature.

In summary, epitaxial $EBTO_{3-\delta}$ films with different contents of V_O were studied as a model system to investigate the relationship between the content of V_O, microstructure, and dielectric relaxation behavior in ABO_3 perovskite oxide films. It was determined that the off-center displacement of Ti ions in $EBTO_{3-\delta}$ films is enhanced by the introduction of V_O. When an electric field is applied, dipolar defects created by V_O are coupled with the off-centered Ti ions, resulting in the dielectric relaxation behavior [Fig. 5(a)]. Also, the activation energy was determined to increase with an increasing content of V_O [Fig. 5(b)]. The present work provides a comprehensive understanding of how to manipulate and optimize dielectric properties and leakage currents in ABO_3 perovskite oxide films.

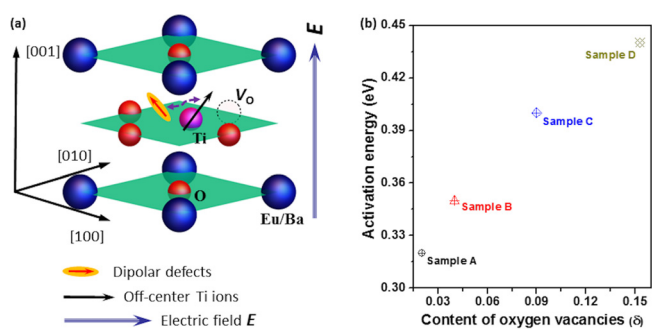

FIG. 5. (a) Schematic diagram of dipolar defects interacting with the off-center Ti ions. (b) The activation energy obtained by fitting dielectric loss-peak as a function of the content of V_O (δ).

See supplementary material for the complete crystal structure, dielectric permittivity, modulus, impedance, and leakage behavior of $EBTO_{3-\delta}$ films.

The authors acknowledge support from the National Natural Science Foundation of China (Grant Nos. U1632122, 11774172, and 11721404) and the Fundamental Research Funds for the Central Universities (Grant Nos. NE2016102 and NP2017103). J.L.M.-D. and W.L. acknowledge support from EPSRC Grant EP/K035282/1, EPSRC Grant EP/N004272/1, and the Isaac Newton Trust [Minute 13.38(k)]. K.H.L.Z. acknowledges financial support from the Chinese Government 1000-Young Talent Program. The oxygen measurement was supported by the Center for Integrated Nanotechnologies (CINT), a DOE nanoscience user facility jointly operated by Los Alamos and Sandia National Laboratories. The STEM study (QH and AYB) was supported by the U.S. Department of Energy (DOE), Office of Science, Basic Energy Sciences, Materials Sciences and Engineering Division. The TEM study at Purdue University was funded by the U.S. National Science Foundation DMR-1643911.

[1]S. B. Oagle, *Thin Films and Heterostructures for Oxide Electronics* (Springer, New York, 2005).
[2]R. Dittmann, "Stoichiometry in epitaxial oxide thin films," in *Epitaxial Growth of Complex Metal Oxides: Techniques, Properties and Application* (Elsevier, 2015).
[3]D. Kan, T. Terashima, R. Kanda, A. Masuno, K. Tanaka, S. Chu, H. Kan, A. Ishizumi, Y. Kanemitsu, Y. Shimakawa, and M. Takano, Nat. Mater. **4**, 816 (2005).
[4]H. Y. Hwang, Nat. Mater. **4**, 803 (2005).
[5]J. F. Schooley, W. R. Hosler, and M. L. Cohen, Phys. Rev. Lett. **12**, 474 (1964).
[6]N. Biškup, J. Salafranca, V. Mehta, M. P. Oxley, Y. Suzuki, S. J. Pennycook, S. T. Pantelides, and M. Varela, Phys. Rev. Lett. **112**, 087202 (2014).
[7]W. D. Rice, P. Ambwani, M. Bombeck, J. D. Thompson, G. Haugstad, C. Leighton, and S. A. Crooker, Nat. Mater. **13**, 481 (2014).
[8]W. W. Li, R. Zhao, L. Wang, R. J. Tang, Y. Y. Zhu, J. H. Lee, H. X. Cao, T. Y. Cai, H. Z. Guo, C. Wang, L. S. Ling, L. Pi, K. J. Jin, Y. H. Zhang, H. Wang, Y. Q. Wang, S. Ju, and H. Yang, Sci. Rep. **3**, 2618 (2013).
[9]J. F. Scott and M. Dawber, Appl. Phys. Lett. **76**, 3801 (2000).
[10]M. Choi, F. Oba, and I. Tanka, Phys. Rev. Lett. **103**, 185502 (2009).
[11]W. W. Li, Q. He, L. Wang, H. Z. Zeng, J. Bowlan, L. S. Ling, D. A. Yarotski, W. R. Zhang, R. Zhao, J. H. Dai, J. X. Gu, S. P. Shen, H. Z. Guo, L. Pi, H. Wang, Y. Q. Wang, I. A. Velasco-Davalos, Y. J. Wu, Z. J. Hu, B. Chen, R.-W. Li, Y. Sun, K. J. Jin, Y. H. Zhang, H.-T. Chen, S. Ju, A. Ruediger, D. N. Shi, A. Y. Borisevich, and H. Yang, Phys. Rev, B **96**, 115105 (2017).
[12]M. Janousch, G. I. Meijer, U. Staub, B. Delley, S. F. Karg, and B. P. Andreasson, Adv. Mater. **19**, 2232 (2007).
[13]S. Lee, A. Sangle, P. Liu, A. Chen, W. Zhang, J. S. Lee, H. Wang, Q. X. Jia, and J. L. MacManus-Driscoll, Adv. Mater. **26**, 6284 (2014).
[14]Y. Teraoka, H. M. Zhang, S. Furukawa, and N. Yamazoe, Chem. Lett. **14**, 1743 (1985).
[15]Y. Teraoka, H. M. Zhang, K. Okamoto, and N. Yamazoe, Mater. Res. Bull. **23**, 51 (1988).
[16]K. Uchino, Ferroelectrics **151**, 321 (1994).
[17]M. Schumacher, G. W. Dietz, and R. Waser, Integr. Ferroelectr. **10**, 231 (1995).
[18]G. A. Samara, J. Phys.: Condens. Matter **15**, R367 (2003).
[19]A. A. Bokov and Z.-G. Ye, J. Mater. Sci. **41**, 31 (2006).
[20]O. Bidault, P. Goux, M. Kchikech, M. Belkaoumi, and M. Maglione, Phys. Rev. B **49**, 7868 (1994).
[21]J. G. Wu and J. Wang, J. Am. Ceram. Soc. **93**, 2795 (2010).
[22]Q. Q. Ke, X. J. Lou, Y. Wang, and J. Wang, Phys. Rev. B **82**, 024102 (2010).
[23]Z. Yu, C. Ang, P. M. Vilarinho, P. Q. Mantas, and J. L. Baptista, J. Appl. Phys. **83**, 4874 (1998).
[24]C. Ang, Z. Yu, and L. E. Cross, Phys. Rev. B **62**, 228 (2000).
[25]W.-W. Li, W. Zhang, L. Wang, J. X. Gu, A. Chen, R. Zhao, Y. Liang, H. Z. Guo, R. J. Tang, C. C. Wang, K. J. Jin, H. Wang, and H. Yang, Sci. Rep. **5**, 11335 (2015).
[26]M. Mayer, "SIMNRA user's guide," Technical Report No. IPP 9/113, Max Planck Institut fur Plasmaphysik, Garching, 1997.
[27]M. Mayer, AIP Conf. Proc. **475**, 541 (1999).
[28]P. D. Nellist, *Science of Microscopy* (Springer, New York, 2007).
[29]H. J. Chang, S. V. Kalinin, A. N. Morozovska, M. Huijben, Y.-H. Chu, P. Yu, R. Ramesh, E. A. Eliseev, G. S. Svechnikov, S. J. Pennycook, and A. Y. Borisevich, Adv. Mater. **23**, 2474 (2011).
[30]F. Kremer and A. Schönhals, *Broadband Dielectric Spectroscopy* (Springer-Verlag, Berlin Heidelberg, 2003).
[31]C. Verdier, F. D. Morrision, D. C. Lupascu, and J. F. Sccot, J. Appl. Phys. **97**, 024107 (2005).
[32]S. Panteny, R. Stevens, and C. R. Bowen, Ferroelectrics **319**, 199 (2005).
[33]C. R. Bowen and D. P. Almond, Mater. Sci. Technol. **22**, 719 (2006).
[34]R. Zhao, W.-W. Li, L. Chen, Q. Q. Meng, J. Yang, H. Wang, Y. Q. Wang, R. J. Tang, and H. Yang, Appl. Phys. Lett. **101**, 102901 (2012).
[35]W.-W. Li, R. Zhao, R. J. Tang, A. P. Chen, W. R. Zhang, X. Lu, H. Wang, and H. Yang, ACS Appl. Mater. Interfaces **6**, 5356 (2014).
[36]Y. Imry and M. Wortis, Phys. Rev. B **19**, 3580 (1979).
[37]W. Kleemann and A. Klossner, Ferroelectrics **150**, 35 (1993).
[38]S. M. Yang, S. J. Moon, T. H. Kim, and Y. S. Kim, Curr. Appl. Phys. **14**, 757 (2014).
[39]M. Dutta, Y. Ding, J. H. Chen, C. L. Chen, A. Bhalla, and R. Y. Guo, Scr. Mater. **130**, 119 (2017).
[40]H. Schremmer, W. Kleemann, and D. Rytz, Phys. Rev. Lett. **62**, 1896 (1989).
[41]D. Sommer, D. Friese, W. Kleemann, and D. Rytz, Ferroelectrics **124**, 231 (1991).
[42]A. Klossner, U. A. Leitao, W. Kleemann, and D. Rytz, Ferroelectrics **157**, 245 (1994).
[43]M. D. Glinchuk, L. Jastrabik, and V. A. Stephanovich, Physica B **222**, 182 (1996).